

K2 study of the Magnetic Precataclysmic Variable V1082 Sagittarius

GAGIK TOVMASSIAN,¹ PAULA SZKODY,² RICARDO YARZA,³ AND MARK KENNEDY⁴

¹*Instituto de Astronomía, Universidad Nacional Autónoma de México, Apartado Postal 877, Ensenada, Baja California, 22800 México*

²*Department of Astronomy, University of Washington, Box 351580, Seattle, WA 98195, USA*

³*Instituto Tecnológico y de Estudios Superiores de Monterrey, 64849 Monterrey, N.L., México*

⁴*Jodrell Bank Centre for Astrophysics, School of Physics and Astronomy, The University of Manchester, Manchester M13 9P*

ABSTRACT

We present a long-term light curve of the precataclysmic variable (CV) V1082 Sgr obtained by the *K2*-mission over the course of 81 days. We analyze the entire complex light curve as well as explore several sections in detail with a sliding periodogram. The long dataset allows the first detection of the orbital period in the light curve, as well as the confirmation of cyclical variability on a longer timescale of about a month. A portion of the light curve in deep minimum reveals a clean, near-sinusoidal variability attributed to the rotation of the spotted surface of the donor star. We model that portion of the light curve assuming that the donor star grossly under-fills its Roche lobe, has cool spots similar to a chromospherically active, slightly evolved early K-star, and might be irradiated by the X-ray beam from the magnetically accreting white dwarf. The fast variability of the object in the active phases resembles the light curves of magnetic CVs (polars).

Keywords: (stars:) novae, cataclysmic variables – stars: individual (V1082 Sgr)

1. INTRODUCTION

Cataclysmic Variables (CVs) are interacting close binary systems consisting of a red star filling its corresponding Roche lobe and losing matter to a white dwarf (WD) companion (Warner 1995). In systems with a strongly magnetic WD the matter falling into the potential well of the WD is captured and channeled onto the magnetic pole(s). There are also a handful of binaries known as prepolars, which are considered as part of the CV family, as there is evi-

dence of accretion onto the WD in these systems (Webbink & Wickramasinghe 2005; Schmidt et al. 2005). All of them contain late M dwarfs, and the orbital periods of the systems are comparable to typical orbital periods for CVs (i.e. less than 6 hr).

However, where the prepolars differ dramatically from CVs is in their accretion rates. Prepolars have been observed to accrete at a rate that is two orders of magnitude less than the typical rate in CVs. In fact, prepolars are technically not CVs, since the accretion geometry in CVs typically requires the secondary to be overflowing its Roche lobe, while prepolars are

detached binaries. Instead, accretion in prepolars is assumed to arise from a coupling of the magnetic fields of both stars in the binary that draws matter lost by the wind from the donor star to accrete onto the magnetic pole of the WD (Wheeler 2012; Ferrario et al. 2015). There should be counterparts of prepolars with donors of earlier spectral types. So far, only two or three candidates have been proposed and the jury is still out as to whether these systems are truly prepolars (Robinson et al. 1988; Tovmassian et al. 2017).

The *K2* mission commenced after the original *Kepler* mission was terminated for technical reasons (Howell et al. 2014). It provides precision photometry of fields concentrated around the ecliptic plane. *K2* provides data at long 30 m and short 1 m cadences over ~ 80 day intervals with precision close to that of the original *Kepler* mission. We proposed observations of V1082 Sgr, an object that demonstrates a large amplitude variability on very different time scales (Tovmassian et al. 2016). Previous long-term photometry revealed that the system is active, or bright most of the time with occasional deep minima. The variability appears to be quasiperiodic with cycles roughly 29 days long. No definite periodicities were found at that or shorter periods. The orbital period of 20.82 hr was determined from the spectroscopic analysis of radial velocity (RV) variations (Thorstensen et al. 2010). The orbital period is well above the 0.4 day upper limit at which a zero age main sequence red dwarf would be filling its corresponding Roche lobe in a binary with an average mass WD primary. The donor star is clearly visible at 50 – 100% of the total flux around 5000 Å depending on the accretion activity state.

Although the object often shows strong emission lines resembling a CV, only a spectrum of a K 2 star is visible in the optical range during the times of minima with a lack of additional ra-

diation in the continuum or spectral lines. This further supports the idea that the companion is underfilling its Roche lobe, as these minima are difficult to explain with a Roche lobe overflowing scenario. However, the precise determination of spectral and particularly the luminosity class of the donor star based on the low-resolution and highly variable spectra was inconclusive.

The secondary is chromospherically active as can be inferred from the presence of narrow H_α and Ca II emission lines (Tovmassian et al. 2016) when the accretion is halted. When the accretion turns on, the emerging strong emission lines are symmetric and of low RV suggesting that they are not formed in an accretion stream characteristic to ordinary polars. Hence, Tovmassian et al. (2016, 2017) suggest that V1082 Sgr is a prime candidate for one of the hard sought detached binaries with a magnetic WD and a magnetically active K-star.

V1082 Sgr has also been studied at X-ray wavelengths by Bernardini et al. (2013) who showed that V1082 Sgr is highly variable in X-rays, with variations on a wide range of time scales from hours to months. The length of the observation was not sufficient to cover the unusually long orbital period of the system. However, Tovmassian et al. (2016) showed that the observed X-ray flare may be related to a changing viewing angle of the accretion column over the orbital period during one of the system's accretion driven stages. A complex fit to the X-ray spectrum reinforces the proposition that the plasma reaches typical temperatures achieved in a magnetically confined accretion flow, where a standing shock is formed at the poles of a compact star.

Here we present the analysis of *K2* observations of V1082 Sgr, which provides new information on the accretion process in this system and adds to the evidence for the magnetic nature of the binary. Some parallels with the X-ray results can be drawn.

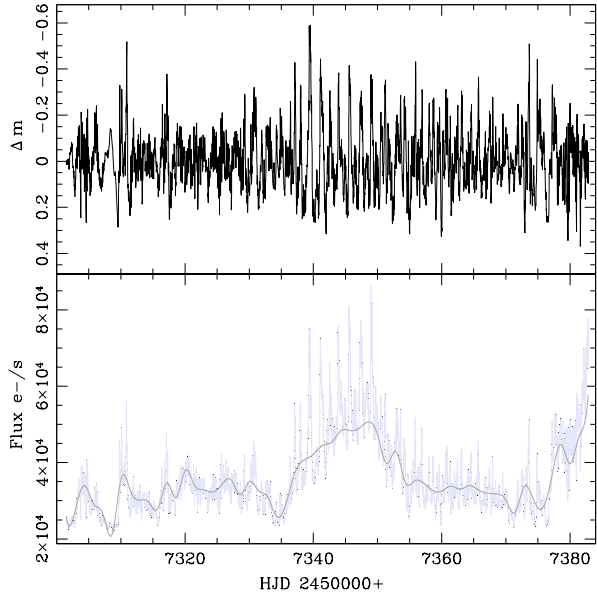


Figure 1. Light curve of V1082 Sgr. Bottom panel: the individual measurements are plotted as tiny dots, connected by thin line. The thick line is a cubic polynomial fit to the data. Top panel: the residual light curve after subtraction of the fit and converted to a logarithmic scale.

2. OBSERVATIONS

V1082 Sgr was observed by the *Kepler* spacecraft as part of Campaign 7 of the *K2* mission from 2015 October 4 to December 26 (BJD = 245 57301.4 – 57382.8; MJD 2467.2 – 2549.8). The integration time of the *Kepler* spacecraft is 6.02 s. Since it is unfeasible to save every single data point taken of an object with this short an integration time (due to the limitations of bandwidth when downloading data from the spacecraft), *Kepler* data are averaged over two different time spans – short cadence and long cadence. For short cadence data, exposures are averaged over approximately 1 minute, while long cadence data correspond to 30 minutes of data. As such, the short cadence data can be treated as a subset of long cadence data, since they are both derived from the same set of 6 s exposures.

We obtained both long and short cadence data (exposures of 29.4 m and 58.8 s respectively) for V1082 Sgr. The data are in the form of integrated photoelectrons collected during either a one or 30 m observation. Each data point in the time series is the direct sum of counts within a predefined aperture. The apertures are constructed to maximize the signal-to-noise ratio of the light curves and take into account the varying pixel response function across the focal plane (Bryson et al. 2010).

The light curves obtained by the in-house pipeline reduction were downloaded from the Mikulski Archive for Space Telescopes. For the short cadence light curve we acquired data processed by the Everest pipeline (Luger et al. 2016) which aims to increase the precision of the photometry designed for exoplanet detection. However we found that the procedure misinterpreted the overall variability of the object and treated them as undesirable trends, removing features which we believe are part of the intrinsic variability of this peculiar binary. Hence, we use in the following analysis the raw fluxes corresponding to the SAP_FLUX in the long cadence dataset. In general, the variability demonstrated by this object far exceeds the stringent precision limits of the *Kepler/K2* mission, designed to detect microvariability produced by transient extra-solar planets. The initial 1.2 days of data, as well as outliers found upon visual inspection as not belonging to the intrinsic variability of the object, were removed.

Additional 40 day monitoring of the object was obtained with the 1.5 m telescope of Observatorio Astronómico Nacional at San Pedro Mártir (OAN SPM) equipped with the RATIR instrument (Butler et al. 2012; Watson et al. 2012) and operating robotically. The data were acquired in Bessel-V and near-IR *J* and *H* bands and differential photometry was used to obtain the final magnitudes. An automatic pipeline procedure implemented in python was

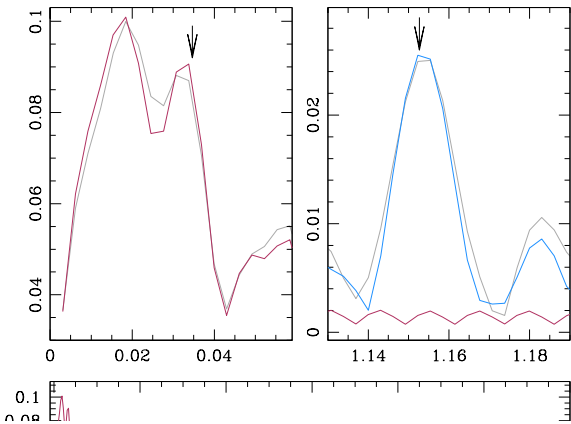


Figure 2. Power spectra of the polynomial fit to the light curve (red curve) and to the residual light curve (blue curve) are presented in the bottom panel. The zoomed-in portions of the power spectra with prominent peaks are presented in upper panels. The arrow in the upper left panel indicates 29 days cyclical variability of the object. The arrow in the upper right panel corresponds to the spectroscopic orbital period of the binary. The gray curve on both of the top panels represents a power spectrum of the original observed light curve. The frequency is in days^{-1} .

used to perform preliminary tasks of bias subtraction, flat-fielding, and cosmic-ray removal. The pipeline also conducts astrometric calibration and sky subtraction for infrared (IR) images. Aperture photometry was done using IRAF *aphot* package (Tody 1986). For more detailed information on these and simultaneous spectroscopic observations see Tovmassian et al. (2018, hereafter Paper II)

3. LONG CADENCE DATA

In the bottom panel of Figure 1 we present the *K2* long cadence light curve of the object. Individual measurements are plotted as tiny dots that are connected to illustrate the rapid, large-scale variability. The light curve shows two intervals of increased brightness, with the second

one cut short by the termination of the observation. In addition to this long-term variability, short-term variability is evident. The amplitude of short-term variability seems to be higher when the overall brightness is higher (8-10% versus 12-18%). We fitted the light curve with a high-order polynomial (cubic spline), shown as a thick curve in the same panel, in order to separate long-term and short-term variability. The high-amplitude and high-frequency peaks were excluded from the fit to study the underlying gross variability. The polynomial order was selected to eliminate all variability over 0.33 c/day frequency (corresponding to 3 days periodicity). The result of the subtraction of the fit from the original data is shown in the top panel of Figure 1 converted to a logarithmic scale.

The fit and the residuals were subjected to period analysis along with the unaltered light curve provided by the *K2* mission. Taking into account the even time distribution of the considered data, a simple discrete Fourier transformation method was used to calculate power spectra (Lenz & Breger 2005). The power spectra are presented in Figure 2. In the bottom panel a range of frequencies is presented in which significant peaks are detected. The red curve is the power spectrum produced by the fit to the data and the blue curve corresponds to the residual light curve containing high-frequency variability. The easily recognizable peaks in the power spectra are the $f_c \approx 0.035$ c/days and $f_c = 1.153$ c/days corresponding to cyclical variability with roughly 29 days recurrence time and orbital period of 20.8 hr, respectively. These peaks are shown in the insets of Figure 2. The black line in the upper panels is the power spectrum calculated with the unaltered light curve, demonstrating that we did not lose any information in the process of separating the low- and high-frequency variability. The orbital period was not detected in the previous ground-based photometry of Tovmassian et al.

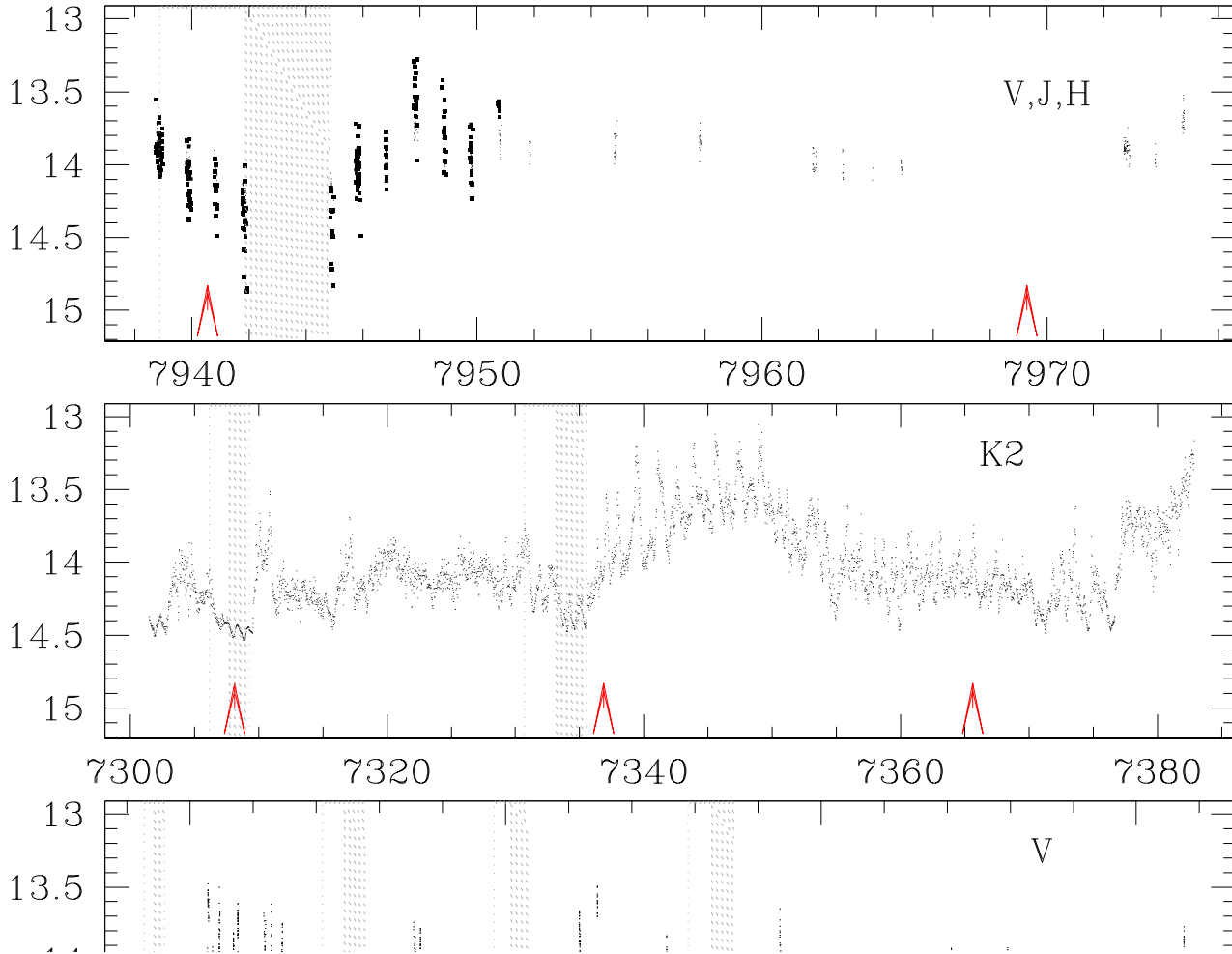


Figure 3. All available photometric observations of V1082 Sgr in different filters. The optical V -band light curve from [Tovmassian et al. \(2016\)](#) is presented in the bottom panel, the K2 light curve in the middle panel, and the new photometric data in V and near-IR J - and H -bands are plotted in the top panel. The magnitudes in y -axes reflect V magnitude and bolder points correspond to the V -band. Light curves in the other two bands are shifted roughly to visually match the former. They are presented to cover a longer time interval and to demonstrate the variable pattern. They are plotted in the same magnitude scale, but the amplitude of variability in IR is smaller, hence they do not precisely overlap. Red arrows indicate moments of minima ~ 29 day cyclical variability calculated from the arbitrary first occurrence. The shaded areas in the bottom and two upper panels indicate actual minima detections.

(2016). The low-frequency peak corresponding to the long-term brightness cycles of the object

is rather strong, although it is based only on 2.8 cycles enclosed within the duration of observations. The strongest peak in the power spectra corresponding to $f = 0.0184$ c/days (54 days) is probably an artifact caused by the brightening of the object around HJD 2457350.

Since the duration of the *K2* observation is certainly not enough to prove the continuity of the 29 day cycles, we combined all of the available photometry of the object in one plot. The composite light curve is shown in the three panels of Figure 3, set in chronological order from bottom to top. In the bottom panel the observations in *V*-band reported in [Tovmassian et al. \(2016\)](#) are plotted, The second panel presents *K2* data converted to *V* magnitudes. The fluxes were converted into magnitudes according to guidelines of the *K2* mission ([Dai et al. 2016](#)). We also use the conversion of *K2* magnitudes to *V* as prescribed by <http://keplerscience.arc.nasa.gov> for a K0 - K5 star by adding a maximum $Kp - V = -0.29$ mag color correction. Bessel-*V* and IR *J*- and *H*-band light curves from RATIR are plotted in the top panel. The *y*-axes of the top panel correspond to magnitudes in the *V*-band with the data plotted as thick points. The *J* and *H* data are over-plotted as tiny points; they were shifted to concur with the *V*-band light curve purposefully to complement it for a longer time interval and underline the general trend.

The full amplitude of variability detected in the previous ground-based observations reaches ≈ 1.5 mag, changing from 13.6 at the maximum to 14.8 mag at the minimum in the *V*-band (bottom panel). A similar scale of variability is observed in the *K2* data, but the variability band is brighter by about 0.3 mag, even after the maximum color correction by 0.29 mag (second from the top). The disparity is a little large for comfort, but apparently there is no direct manner to relate measurements in the

much narrower Johnson filters compared to the *K2* bandpass.

The composite light curve covers over 1000 days. When subjected to a period analysis after normalization of each band to its faintest magnitude, a peak at $f_c = 0.0348$ c/days frequency corresponding to 28.8 days is the strongest. The red arrows The moments of so called "deep minimum" are marked as shaded regions in the plots. This long-term variability is not strictly periodic, and that the brightness of the object does not always reach a deep minimum. The deep minima are short-lived compared to the length of the cycle and their duration is variable (please note that the horizontal scales (*x*-axes) of the panels are significantly different).

Additional coverage from the SPM falls in line with the rest of the accumulated data on the cyclical variability by providing near-IR data. It is not dense enough to explore the orbital variability. The $V - J$ and $J - H$ color calculated around HJD 2457942 from nearly simultaneous exposures are 1.85 ± 0.05 and 0.55 ± 0.04 , respectively. These values correspond to a K3-K4 V star ([Pecaut & Mamajek 2013](#)), which is cooler than K2 determined from the spectral classification ([Tovmassian et al. 2016](#)), but once again confirming that in the deep minima the donor star is the main contributor of light. A possible explanation for the spectral class difference may lie with the IR-excess related to the presence of cyclotron radiation often observed in polars ([Harrison & Campbell 2015](#)), which is beyond the scope of this paper. In the maximum brightness around HJD 2457948 the increase is mostly in the optical light with $V - J$ decreasing to 1.54 ± 0.02 while $J - H$ stays nearly constant. For more on IR magnitudes and color index variability please see Paper II.

4. SHORT CADENCE DATA

The short cadence data are important to explore high-frequency variability. Hence, the low-frequency variability was removed from the

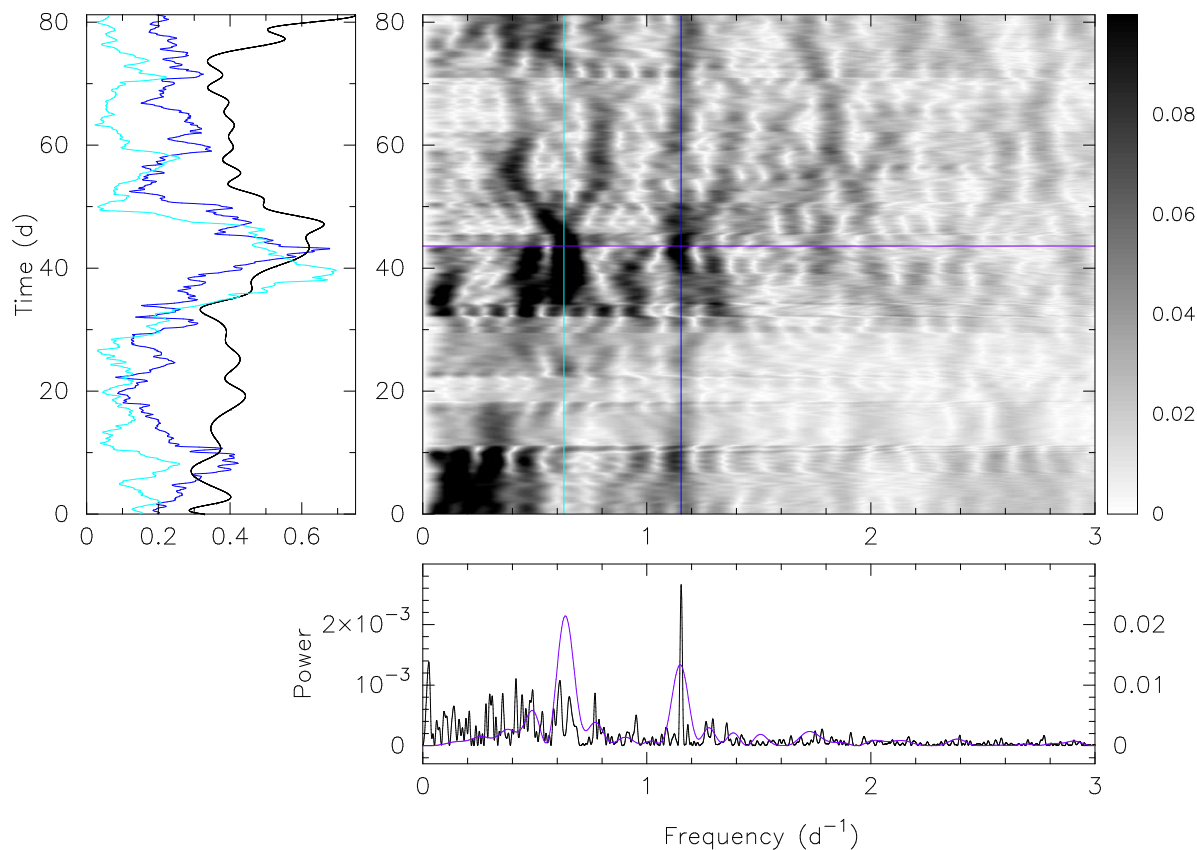


Figure 4. Low-frequency end of the wavelet is presented in the central panel (see text for the description). In the bottom panel the power spectra of the *K2* light curve is presented with a black line. The dark violet line represents the power spectrum corresponding to the cut in the wavelet indicated by the horizontal line of the same color. In the left panel the light curve of the object is plotted with a black line, and the dark and light blue curves correspond to the intensity of frequencies marked by the vertical lines of corresponding colors. The dark blue line corresponds to the orbital frequency, while the light blue is the strongest, but transitional, peak at 0.63 cycles per day frequency.

data by subtracting the corresponding fit similar to the long cadence light curve, as described in the previous section. However, no significant peaks other than those mentioned above are observed in the short cadence data. But, since the amplitude of the variability is changing with the overall brightness of the system, we wanted to check for any possible transient frequencies in the light curve. Considering that the analyzed data is evenly sampled without any time gaps, there was no need to use an elaborate wavelet analysis like one proposed by Foster (1996). Instead, we proceeded with a method known as the “sliding periodogram” described in detail by

Neustroev et al. (2005, and references therein). Thus, we simply divided the entire time series into 857 pieces of 10 day duration, with a 2 hr step following the prescription¹ between individual pieces. We performed a period analysis on each 10-day-long piece and obtained 857 power spectra, which were stacked into a dynamical power density spectrum (DPDS). The DPDS at low frequencies is presented in Figure 4. Any strictly periodic signal must appear as a persistent feature at a constant fre-

¹ in the retrospect, there are no frequencies to explore below 2 hr in the data.

quency in the DPDS. As in the case with a simple periodogram, we could not detect any significant lines. The worm-like features abundant in the DPDS are random super-position of noise in a low-contrast image deprived of a strong signal, and are common in similar situations (Neustroev et al. 2005). Several features, however, are eye-catching. The orbital period is seen throughout the entire dataset, but the signal is much stronger when the system is bright. In the central panel of Figure 4 depicting low frequencies, the dark blue vertical line indicates the orbital frequency. In the bottom panel, the power spectrum of the entire dataset is shown by the black line and a power spectrum obtained close to the peak brightness of the object by a violet line. That occasion is indicated by a horizontal violet line in the central panel. There is a strong transient signal at 0.63 cycles/day in that part of the light curve, exceeding the orbital period. In the left panel the black line is the polynomial fit to the light curve, the violet is the amplitude of the signal at the orbital frequency, and the cyan is the amplitude of the $f_{0.63}$ frequency. We have no explanation whether this periodicity is real and why it appears at the height of the brightness. Certainly the light curve at that stretch of time is better described by the presence of both frequencies as can be seen in Figure 5. Here the violet dotted line is the Fourier component at the orbital period and the light blue line is the sum of both. During several nights the light curve is seen as having bimodal frequency. A modulation due to two-pole accretion on the WD hardly can explain that because it can modify the phase and the amplitude, but the period should be the same as orbital. We also have to beware that in optical observations of CVs, Warner’s (1989) notes random accretion processes that can produce periodic signals in short time segments.

The speed and amplitude of the variability is not uncommon for magnetic WDs in po-

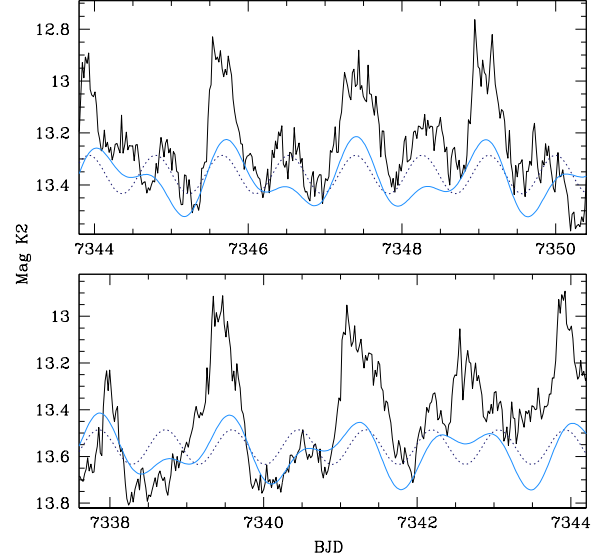


Figure 5. Portion of the light curve where the second, transient $f_{0.63}$ frequency shows up stronger than the orbital period. Apparently there are high-amplitude peaks in the light curve followed by a smaller peaks. Overall, this part of the light curve is better described by a double frequency curve than just orbital one, present throughout the data set. The source of the second frequency is unknown.

lars. In the upper panel of Figure 6 we plotted another arbitrary piece of the light curve of V1082 Sgr selected to match roughly fast ground-based photometry of a known polar IGR J19552+0044 (Tovmassian et al. 2017), shown in the bottom panel. In fact, the photometry of IGR J19552+0044 is faster and the $K2$ light curve of V1082 Sgr looks like a smoothed version of the former.

Finally, the inspection of the wavelet in the higher frequencies (Figure 7) shows just one artifact at $f=11.2$ cycles/day that is relatively strong and persistent. This signal is of interest as there was a transient periodic signal with a frequency of 2 ± 0.14 h detected in X-ray observations of V1082 Sgr (Bernardini et al. 2013) that is close enough to suspect coincidence. This timescale is intriguing as it is of the same order of magnitude as the estimated time it would take matter to travel from the donor

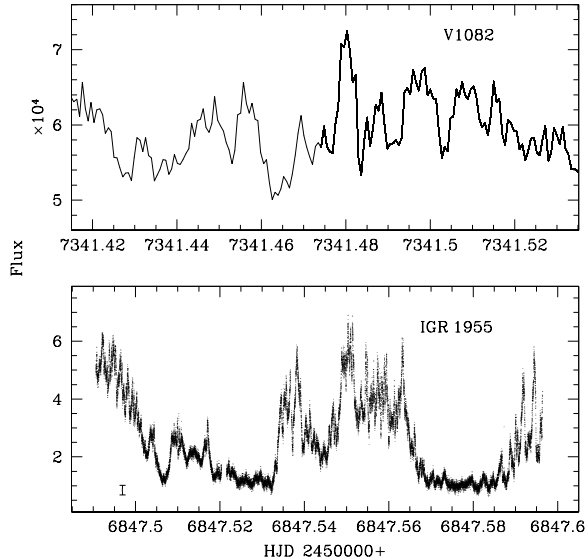


Figure 6. The light curve of V1082 Sgr in the active accretion mode is remarkable for its high-amplitude fast variability (top panel). That is not very unusual, though, considering that the WD accretes the matter on its magnetic pole, similar to polars. In the bottom panel a light curve of polar IGR J19552+0044 (Tovmassian et al. 2017) is presented in a similar time and amplitude scale to demonstrate similarities.

star to the WD. We can claim a marginal detection of the same periodicity. It is the strongest in a time segment when the object is not at the maximum of brightness, but is active.

5. SPOTTING THE DONOR STAR

In the previous section we showed that the orbital period is omnipresent in the data, but often concealed under other large amplitude variability. The most interesting part of the data is related to the minima in which the orbital modulation becomes dominant. There are three episodes related to the 29 day cyclical activity in the *K2* light curve marked with red arrows (see Figure 3). The first one (near BJD 2457308) coinciding with the object reaching the faintest brightness level during 80 days, is of particular interest. Figure 8 shows a portion of the *K2* light curve when the deep minimum occurs. As

the brightness nears its lowest levels, the flickering disappears completely, and the light curve is smooth and near-sinusoidal with a slight downward trend.

A sinusoidal function with a fixed orbital frequency, but variable phase and amplitude, was fit to the small portion of the light curve around the minimum (BJD 7307.5 to 7309.5). The best fit model was estimated using a Monte Carlo Markov Chain (MCMC) implemented in python using EMCEE (Foreman-Mackey, et al. 2013). A total of 20 walkers were used with 25000 steps allowed, and the first 5000 steps were discarded as burn-in. Flat priors were assumed for the amplitude, phase, and offset. The best-fit model is shown in the top panel of the inset in Figure 8. In the inset’s lower panel the RV curve corresponding to the donor star is plotted according to the precise RV measurements of recent high-resolution spectroscopic observations (Paper II). The ephemeris derived from the RV data predicts that minimum light when the light curve is dominated by the secondary star should be at orbital phase 0.25 (marked as dashed lines in the inset). However, the best-fit phase from the MCMC analysis was 0.3172 ± 0.0001 , which corresponds to a phase shift of 0.0672 ± 0.0001 , relative to the RV ephemeris. This error is dominated by the errors on the *Kepler* data, and is likely too small given that the light curve is not perfectly sinusoidal. To account for this, we re-did the MCMC analysis, but also allowed for a scaling factor on the error of the data with a Jeffreys prior (that is, $P(\sigma) \propto \frac{1}{\sigma}$). The resulting best-fit phase was 0.32 ± 0.03 at the 3σ level, which corresponds to a phase shift of 0.07 ± 0.03 relative to the RV ephemeris.

In the deep minimum, like the one achieved in the selected portion of the light curve, the predominant source of light has to be the donor star. It can be safely assumed that the flickering is associated with the ongoing accretion, and that its disappearance indicates suspension

of accretion-related radiation. V1082 Sgr was observed spectroscopically over extended periods of time, and on several occasions it showed significant weakening of emission-line intensities simultaneously with the fading of the brightness (continuum). During short instances, only a very narrow faint chromospheric H_α line is detected, indicating a total cessation of accretion fueled ionization (Tovmassian et al. 2016), while the continuum corresponds to a K-star in the entire optical range. These observations lead to an important conclusion that the light from the donor star in this binary varies with the orbital period with an amplitude of 0.08 mag amplitude.

6. ESTIMATES AND DISCUSSION

Detection of a single-humped, smooth, almost sinusoidal wave from the donor star in a compact binary means that the star’s rotation is synchronized with the orbital period. Even more importantly, it means that the donor star is not ellipsoidally deformed, i.e, does not fill its Roche lobe. In a Roche lobe overflowing long-period CV, in which the secondary star contributes significantly to the light, the variability is double-humped and usually uneven, like in V630 Cas (see Fig 5 Orosz et al. 2001). This confirms our earlier interpretation of V1082 Sgr as a detached binary (Tovmassian et al. 2017).

The variability then is a result of a spot covering a large fraction of the stellar surface to produce the observed amplitude of the light curve. It is typical of a fast rotating K-type dwarf in the form and the amplitude (e.g. AB Dor Anders et al. 1992). So, the natural assumption is that the variability is caused by a a cool spot commonly observed in chromospherically active K stars. An alternative explanation could be a possible heated/irradiated face (the side permanently facing the WD) of the donor star. The expected phase shift in such a case between the RV zero point and the light curve extrema should be 0.25, instead of the observed 0.32 P_{orb}

range. At this point it is difficult to say if this difference is significant enough to discard the latter possibility.

Nevertheless, we used a binary star modeling tool, Nightfall (Wichmann 2011), to check for possible solutions. Two and a half orbits of data with changing profile of the variability is not sufficient for a serious modeling attempt, hence we do not really fit the light curve. Instead, in Figure 9 we present the same fraction of the light curve, as in the inset of Figure 8, by overplotting possible solutions offered by Nightfall. Input parameters of the binary used to produce this light curve are listed in Table 1. They were deduced largely using the X-ray spectral fit (Bernardini et al. 2013) for the estimate of WD mass and the analysis of high-resolution spectroscopy in regard to the parameters of the donor star (see details in Paper II).

The probe confirms that employing a fill factor > 0.7 immediately produces double humps in the light curve, even for such a low inclination of the orbital plane as $i = 23^\circ$. The only viable solutions to reproduce the observed light curve involve a rather spherical star with spot(s).

The red symmetric curve in Figure 9 is produced by adding a heated spot in the front of the star. It resembles the first full orbit at the deep low state between BJD 7308 – 7309. However, there is a "knee" on the receding wing of the light curve, which is much stronger in the second orbit between BJD 7309 -7309.6 after which the system suddenly brightens up. The blue model (the blue curve in Figure 9), which was calculated by adding a cool spot at the back of the K-star, seems to work better to explain the asymmetric wing. The problem is not only with the symmetry. In order to place the minimum light 0.06 orbital phases prior to the conjunction (corresponding to the orbital phase 0.0), the heated spot should be displaced from the center of the line connecting stellar components by as much as 35° in longitude. To make it

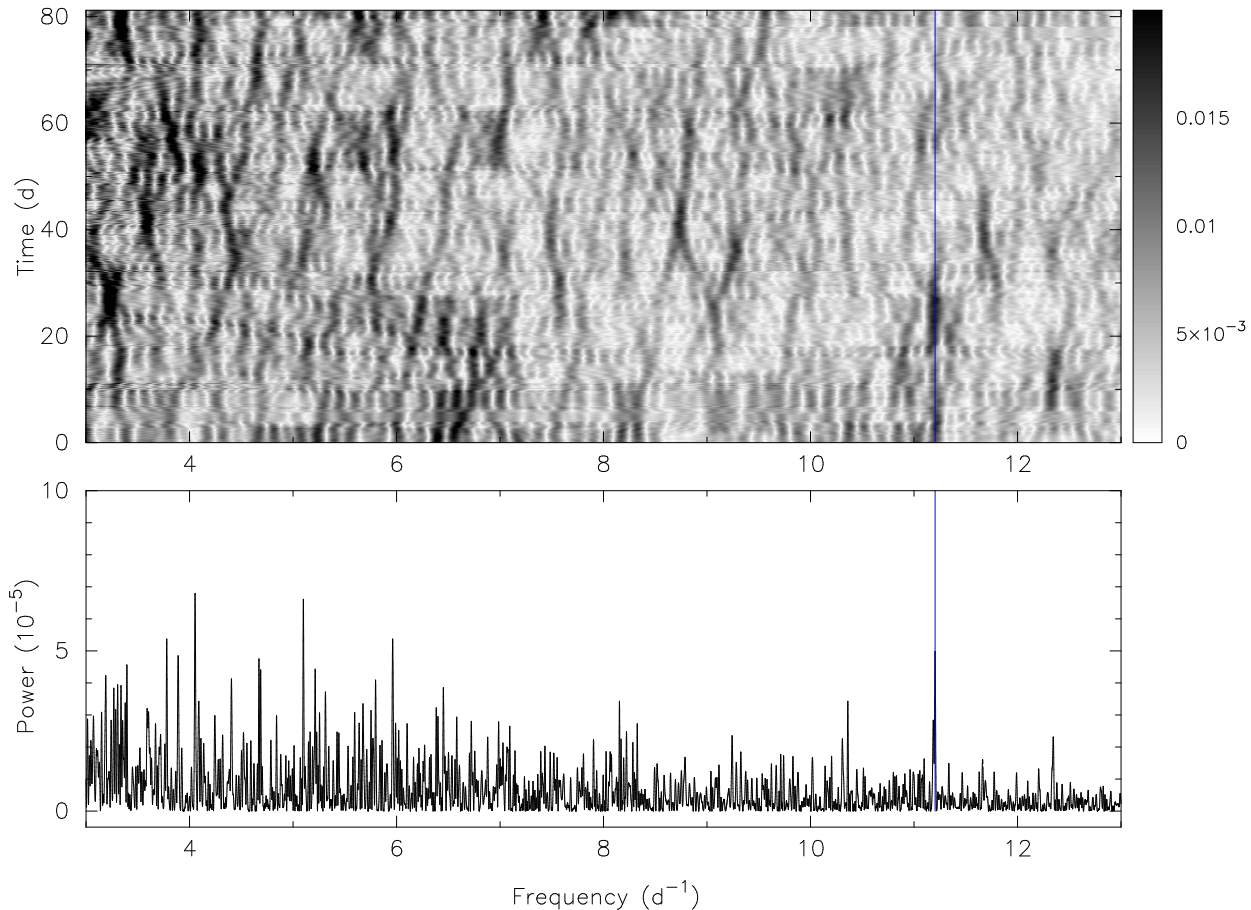


Figure 7. Higher frequency portion of the wavelet. The strongest peak in this portion (two orders of magnitude smaller than the orbital frequency) is at around 4 cycles/day. It is most likely an alias produced by the thruster firings of the *K2* satellite (Van Cleve et al. 2016). The other relatively strong and persistent peak is at 11.2 cycles/day. This one is remarkable for its possible counterpart in X-ray data (Bernardini et al. 2013). No other definitive frequencies are observed.

wide enough, the heated spot has a $\sim 50^\circ$ deg radius, which is not really realistic. In contrast, the cool spot should not necessarily be aligned with anything and does not have to be round or symmetrical. It also can be variable in size and intensity.

We think that a cool spot is a more reasonable solution to explain the observed variability of the K-star. The parameters of the cool spot in the presented model assume a spot that is 370 K cooler than the effective temperature of the star. The spots in such active stars can be really long lived, but they evolve and patterns change. Usually, the spots are neither single nor round. So the stellar surface cannot be accurately modeled based on the short duration

of deep minima. Neither can a combination of a hot spot with a cool one be excluded. We only attempted to show that a spot assumption is realistic in terms of its size and temperature difference.

7. CONCLUSIONS

We explored an unprecedented 80-day-long uninterrupted light curve of the enigmatic binary V1082 Sgr with high time resolution obtained by the *K2* mission. This is impossible using ground-based telescopes, with the long 0.867 d orbital period of the binary and ~ 29 days cyclical variability. We identified the orbital variability in the light curve known previously from spectroscopy. We also observe

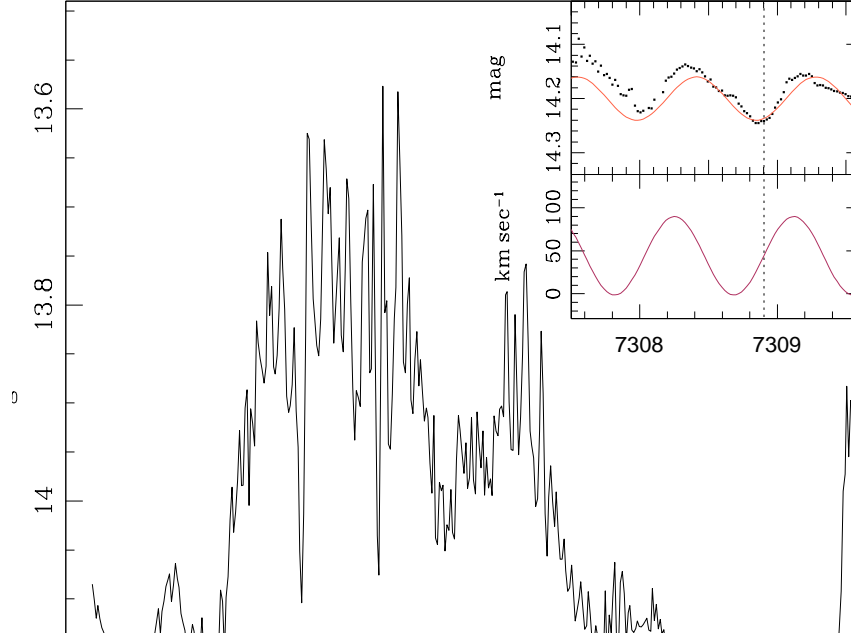


Figure 8. Another portion of the light curve of the short active accretion period flanked by two deep minima. The one at the right side starting around BJD 7307.5 is particularly remarkable. It is the lowest brightness observed in 80 days of monitoring and lasting 2.5 orbits (~ 50 hr). The curve is smooth, without signs of accretion flickers, and is clearly modulated with the orbital period. The orbital period is shown as a light red sinusoid fitted to that small portion of the light curve, presented in the inset of the figure in the upper panel. In the bottom panel of the inset a radial velocity curve from spectroscopic observations is plotted (Paper II). The conjunction of stellar components is marked by a dotted vertical line.

cyclical, quasiperiodic minima in the light curve in the *K2* data, as well as in the follow-up ground based photometry. The minima usually are brief, lasting two or three orbital periods, followed by a sudden and strong increase of the brightness. When the system is active it exhibits fast, large amplitude variability resembling ordinary magnetic CVs or polars. Some transient periods are seen in the active phase, for which there are no ready explanations. The ~ 2 hr transient period that has been observed in X-rays is marginally detected in the optical light curve.

The only persistent, and strictly periodic signal is the orbital one, revealed in both active accretion and accretion-shutdown states. In the active state the signal at the orbital frequency is strong, indicating modulation of the accretion process similar to polars. The period is coherent throughout the entire 80 day dataset.

In the low brightness state the orbital period persists and is clearly visible. Spectroscopic and photometric observations and the spectral energy distribution show that during this interval nearly all of the light comes from the K 2 star. Detection of a smooth orbital variability during the deep minimum confirms the absence of

Table 1. Binary parameters used in the Nightfall

Inclination	23.0	(degree)	
Mass Ratio	0.88		
Period	0.867	(days)	
Total Mass	1.37	(solar mass)	
Separation	4.25	(solar radius)	
	Donor	WD	
Amp. RV	45.35	51.5	(km/s ⁻¹)
Mass	0.73	0.64	(solar mass)
Mean Radius	1.1	0.015	(solar radius)
Fill Factor	0.67	0.01	
Temperature	4930.0	30000.0	(Kelvin)
Asynchronicity	1.0	1.0	
Albedo	0.5	1.0	
Grav. Dark.	0.107	0.25	
Spot on the	donor	star	
Long.	Lat.	Radius	DimFactor
145.0	0.0	50.0	0.925

accretion, as the latter is usually accompanied with fast spikes in the light curve. The form of the light curve suggests that the K-star is not ellipsoidally shaped. The duration of this nonaccreting state is not long and has not been observed repetitively with sufficient time resolution in order to provide an observational base for serious modeling. However, we demonstrate qualitatively that it can simply be a result of a large cool spot on the surface of a chromospheric K-star.

The orbital variability could also be produced by a hot spot formed as a result of irradiation. The reality can be more complex with both hot and cool spots present.

Regardless of the origin of spot(s), the light from the K-star modulated with the orbital period means that the K-star rotates synchronously with the binary system. The form of the variability indicates an absence of deformation associated with the star filling its Roche lobe. These are the two the most important re-

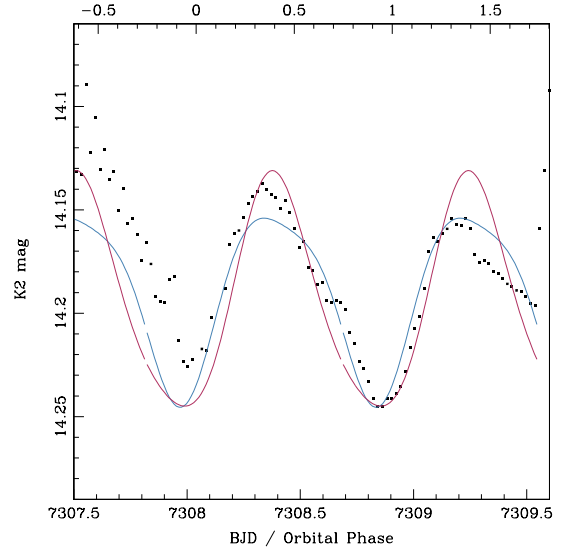


Figure 9. Light curve of the object at the deep minimum around BJD 7308.5. Black points are observational data and the red curve is a binary model with hot spot on the face of the donor star (slightly shifted from line connecting the stars). The blue line is a model with a cool spot on the surface of the donor star. The models are not fits to the actual observations, they are just made to qualitatively correspond to the shape of the light curve and amplitude. See the text for explanations.

sults from our analysis of the *K2* observations. Paper II pairs these conclusions with the mass of the WD determined from the X-ray observations and the results of the high-resolution spectroscopy to further the interpretation of this interesting system.

G.T. acknowledges PAPIIT grants IN108316 and CONACyT grant 166376. P.S. acknowledges NSF grant AST-1514737. M.R.K. is funded through a Newton International Fellowship provided by the Royal Society.

Facilities: Kepler-K2, OAN SPM (RATIR)

Software: IRAF, Everest, Nightfall, Period04

REFERENCES

- Anders, G. J., Coates, D. W., & Thompson, K. 1992, *Proceedings of the Astronomical Society of Australia*, 10, 33
- Bernardini, F., de Martino, D., Mukai, K., et al. 2013, *MNRAS*, 435, 2822
- Bryson, S. T., Tenenbaum, P., Jenkins, J. M., et al. 2010, *ApJL*, 713, L97
- Butler, N., Klein, C., Fox, O., et al. 2012, *Proc. SPIE*, 8446, 844610
- Dai, Z., Szkody, P., Garnavich, P. M., & Kennedy, M. 2016, *AJ*, 152, 5
- Ferrario, L., de Martino, D., & Gänsicke, B. T. 2015, *SSRv*, 191, 111
- Foreman-Mackey, D., Hogg, D. W., Lang, D., et al. 2013, *Publications of the Astronomical Society of the Pacific*, 125, 306.
- Foster, G. 1996, *AJ*, 112, 1709
- Harrison, T. E., & Campbell, R. K. 2015, *ApJS*, 219, 32
- Howell, S. B., Sobeck, C., Haas, M., et al. 2014, *PASP*, 126, 398
- Lenz, P., & Breger, M. 2005, *Communications in Asteroseismology*, 146, 53
- Luger, R., Agol, E., Kruse, E., et al. 2016, *AJ*, 152, 100
- Neustroev, V. V., Zharikov, S., Tovmassian, G., & Shearer, A. 2005, *MNRAS*, 362, 1472
- Orosz, J. A., Thorstensen, J. R., & Kent Honeycutt, R. 2001, *MNRAS*, 326, 1134
- Pecaut, M. J., & Mamajek, E. E. 2013, *ApJS*, 208, 9
- Robinson, E. L., Clemens, J. C., & Hine, B. P. 1988, *ApJL*, 331, L29
- Schmidt, G. D., Szkody, P., Vanlandingham, K. M., et al. 2005, *ApJ*, 630, 1037
- Thorstensen, J. R., Peters, C. S., & Skinner, J. N. 2010, *PASP*, 122, 1285
- Tody, D. 1986, *Proc. SPIE*, 627, 733
- Tovmassian, G., González-Buitrago, D., Zharikov, S., et al. 2016, *ApJ*, 819, 75
- Tovmassian, G., González-Buitrago, D., Thorstensen, J., et al. 2017, *A&A*, 608, A36
- Tovmassian, G., Gonzalez-Buitrago, D., & Zharikov, S. 2017, 20th European White Dwarf Workshop, 509, 489
- Tovmassian, G., Gonzalez, J.F., Hernandez, M.S., Gonzalez-Buitrago, D., Zgarikov, S., Hernandez Santisteban, J.V., 2018, submitted to *ApJ*
- Van Cleve, J. E., Howell, S. B., Smith, J. C., et al. 2016, *PASP*, 128, 075002
- Warner, B. 1989, *Information Bulletin on Variable Stars*, 3383, 1
- Warner, B. 1995, *Camb. Atmos. Space Sci. Ser*, 5
- Watson, A. M., Richer, M. G., Bloom, J. S., et al. 2012, *Proc. SPIE*, 8444, 84445L
- Webbink, R. F., & Wickramasinghe, D. T. 2005, *The Astrophysics of Cataclysmic Variables and Related Objects*, 330, 137
- Wheeler, J. C. 2012, *ApJ*, 758, 123
- Wichmann, R. 2011, *Astrophysics Source Code Library*, ascl:1106.016